

# Cosmological dynamics with propagating Lorentz connection modes of spin zero

**Hsin Chen<sup>a</sup>, Fei-Hung Ho<sup>a</sup>, James M. Nester<sup>a,b,c</sup>,  
Chih-Hung Wang<sup>a</sup>, Hwei-Jang Yo<sup>d</sup>**

<sup>a</sup>Department of Physics, National Central University,  
No. 300, Jhongda Rd., Jhongli 320, Taiwan

<sup>b</sup>Institute of Astronomy, National Central University,  
No. 300, Jhongda Rd., Jhongli 320, Taiwan

<sup>c</sup>Center of Mathematics and Theoretical Physics, National Central University,  
No. 300, Jhongda Rd., Jhongli 320, Taiwan

<sup>d</sup>Department of Physics, National Cheng-Kung University,  
No. 1, University Rd., Tainan 701, Taiwan

E-mail: hchen@ntnu.edu.tw, 93242010@cc.ncu.edu.tw, nester@phy.ncu.edu.tw,  
chwang@phy.ncu.edu.tw, hjyo@phy.ncku.edu.tw

**Abstract.** The Poincaré gauge theory of gravity has a Lorentz connection with both torsion and curvature. For this theory two good propagating connection modes, carrying spin-0<sup>+</sup> and spin-0<sup>-</sup>, have been found. The possible effects of the spin-0<sup>+</sup> mode in cosmology were investigated in a previous work by our group; there it was found that the 0<sup>+</sup> mode could account for the presently accelerating universe. Here, we extend the analysis to also include the spin-0<sup>-</sup> mode. The resulting cosmological model has three degrees of freedom. We present both the Lagrangian and Hamiltonian form of the dynamic equations for this model, find the late-time normal modes, and present some numerical evolution cases. In the late time asymptotic regime the two dynamic modes decouple, and the acceleration of the Universe oscillates due to the spin-0<sup>+</sup> mode.

PACS numbers: 04.50.-h, 04.50.Kd, 98.80.Cq, 98.80.Jk

## 1. Introduction

This work reports on an extension of a certain cosmological model, based on the Poincaré gauge theory of gravity (PGT), which was first announced in [1] and then presented in considerable detail in [2]. In the latter work it was shown that the dynamic Riemann-Cartan geometry (with curvature and torsion) could contribute an oscillating aspect to the Universe expansion which could account for the present day observed acceleration. Since then two new works have appeared analyzing the dynamics of this model and addressing its fit to the cosmological observations [3, 4]. These works have already covered many features of the original model in considerable detail. Here we wish to first review the results of the application of certain theoretical principles to the PGT. That will naturally lead us to a more appropriate description and our extension of the original model.

One of the outstanding successes of theoretical physics in the latter part of the last century which led to a much deepened understanding was the recognition that all the known fundamental physical interactions, the strong, weak, and electromagnetic—*not excepting gravity*—can be well described in terms of a single unifying principle: that of local gauge theory. Although there are other possible gauge approaches, for gravity it seems highly appropriate to regard it a gauge theory for the local symmetry group of Minkowski space time: the Poincaré group [5, 6]. Such a consideration led to the development of the Poincaré Gauge Theory of gravity (PGT) [7, 8, 9, 10, 11, 12]. The PGT has *a priori* independent local rotation and translation gauge vector potentials: the Lorentz (i.e., metric compatible) connection and the orthonormal co-frame; their associated field strengths are the *curvature* and *torsion*. The space-time then has generically a Riemann-Cartan geometry. Because of its gauge structure and geometric properties the PGT has been regarded as an attractive alternative to general relativity.

The theory includes as exceptional cases Einstein’s general relativity (GR) with *vanishing* torsion, the Einstein-Cartan theory with *non-dynamic* torsion algebraically coupled to the intrinsic spin of the source, as well as the teleparallel theories—wherein curvature vanishes but torsion does not. The generic PGT has, in addition to the metric familiar from GR, a connection with some independent dynamics, manifested in both the torsion tensor and additional non-vanishing post-Riemannian curvature components.

Investigations (especially [8, 13]) of the linearized theory have identified six possible dynamic connection modes, carrying certain spins and parity:  $2^\pm, 1^\pm, 0^\pm$ . It is not possible for all of the modes to have good dynamics. The possible combinations of well behaved (carrying positive energy at speed  $\leq c$ ) propagating modes in the linear PGT theory were identified. The Hamiltonian analysis revealed the related constraints [14]. Then detailed investigations of the Hamiltonian and propagation [16, 15, 17, 18] concluded that effects due to nonlinearities in the constraints could be expected to render all of these cases physically unacceptable except for the two “scalar modes”, carrying spin- $0^+$  and spin- $0^-$ .

One mode (referred to as the “pseudoscalar” because of its  $0^-$  spin content) is reflected in the axial vector torsion. Axial torsion is naturally driven by the intrinsic spin of fundamental fermions; in turn it naturally interacts with such sources. Thus for this mode one has some

observational constraints [19, 20]. Note that except in the early universe one does not expect large spin densities. Consequently it is generally thought that axial torsion must be small and have small effects at the present time. The other good mode,  $0^+$ , the so-called “scalar” mode, is reflected in the vector torsion. There is no known fundamental source which directly excites this mode. Conversely this part of the connection does not interact in any direct obvious fashion with any familiar type of matter [21]. Hence we do not have much in the way of constraints as to its magnitude. We could imagine it as having significant magnitude and yet not being dramatically noticed—except indirectly through the non-linear equations.

Thus the theoretical PGT analysis led to just two dynamic Lorentz connection modes. An obvious place where one might see some physical evidence for these modes is in cosmological models. The cosmological homogeneous and isotropic assumptions greatly restrict the possible types of non-vanishing fields. Curiously, for the connection and torsion there are only two possibilities, which reflect precisely the two spin-0 connection modes. The scalar  $0^+$  which gives rise to a special vector torsion which has only a time component, and the pseudoscalar,  $0^-$  mode, which gives rise to an axial torsion which is the dual of a vector with only a time component. Hence the homogeneous and isotropic cosmologies are *naturally* very suitable for the exploration of the physics of the dynamic PGT “scalar modes”.

Thus cosmological models offer a situation where a dynamic Lorentz connection may lead to observable effects. Here we will not focus on the early universe, where one could surely expect large effects (although their signature would have to be disentangled from other large effects), and instead inquire whether one could see any effects of the PGT dynamic connection in the present day universe. In particular we will here consider accounting for the outstanding present day mystery: the accelerated universe, in terms of an alternate gravity theory with an additional natural dynamic geometric quantity: a Lorentz connection [1, 2].

The observed accelerating expansion of the Universe suggested the existence of a kind of dark energy with a negative pressure. The idea of a dark energy is one of the greatest challenges for our current understanding of fundamental physics [22, 23, 24]. Among a number of possibilities to describe this dark energy component, the simplest may well be by means of a cosmological constant  $\Lambda$ . Another popular idea is the quintessence field — some unusual type of minimally coupled scalar field — which has received much attention over the past few years and a considerable effort has been made in understanding the role of quintessence fields on the dynamics of the Universe (see, e.g., [25, 26, 27]).

An alternative is to consider some other gravity theory. Which brings us to our specific topic: the possibility of explaining the accelerating universe using a well tested alternative gravity theory, one well motivated by both geometrical and physical gauge theory principles. We explore the possibility that the dynamic PGT Lorentz connection modes can drive the acceleration of the universe. As noted above, there are two spin-0 modes which could have dynamical behavior. In [2] it was shown that the the spin  $0^+$  mode can make the expansion rate oscillate, naturally having an accelerating expansion in some periods and a decelerating expansion at other times. For suitable choices of parameters and initial data the model can account for the supernova observations. Here we show that including the  $0^-$  mode allows for an improved matching.

Over the years there have been many studies of PGT cosmology, especially by Minkevich and coworkers (see, e.g., [28, 29, 30, 31, 32]). Using various models they found that it was possible for the PGT to avoid singularities, account for inflation, and produce the acceleration of the universe (as discussed later in Section 3, their mechanism is different from that of our dynamic  $0^+$  mode). A comprehensive early survey of the PGT cosmological models was presented quite some time ago by Goenner and Müller-Hoissen [33]. Although that work only solved in detail a few particular cases, it developed the equations for all the PGT cases—including those for the particular model we consider here. However that work was done prior to the discovery of the accelerating universe, and torsion was thus imagined as playing a big role only at high densities in the early universe. More recently investigators have begun to consider various models with torsion as a possible cause of the accelerating universe (see, e.g., [32, 34, 35, 36]).

We have taken another step in the exploration of the possible evolution of the Universe with dynamic Lorentz connection spin-0 modes of the PGT. The main motivation is two-fold: (1) to have a better understanding of the PGT, in particular the possible physics of the dynamic spin-0 modes; (2) to consider the prospects of accounting for the outstanding present day mystery—the accelerating universe—in terms of an alternative gravity theory, more particularly in terms of the PGT. With the usual assumptions of isotropy and homogeneity in cosmology, we find that, under the model, the Universe will oscillate with generic choices of the parameters. The  $0^+$  dynamic mode in the model plays the role of the imperceptible “dark energy”. With a certain range of parameter choices, it can account for the current status of the Universe, i.e., an accelerating expanding universe with a value of the Hubble constant which is approximately the present one. These promising results should encourage further investigations of this model, along with a detailed comparison of its predictions with the observational data.

The remainder of this work is organized as follows: We summarize the formulation of the PGT in general and our model with scalar and pseudoscalar modes in Sec. 2, and then consider the PGT scalar mode cosmological model in Section 3. In Section 4 an effective Lagrangian and Hamiltonian for our cosmological model is presented. This is followed by a late-time asymptotic expansion in Section 4 in which certain normal modes are identified. Section 6 includes the results of our numerical demonstrations for various choices of the parameters and the initial data along with a comparison with the supernova observations. The implications of our findings are discussed in Section 7 and Sec. 8 is a conclusion.

Throughout the paper our conventions are as follows: The spacetime signature is  $(-, +, +, +)$  and  $c = \hbar = 1$ . The Greek indices,  $\alpha, \beta, \gamma \dots$ , are 4d orthonormal (anholonomic) indices, whereas the Latin indices  $i, j, k \dots$  are 4d coordinate (holonomic) indices; they both range over 0, 1, 2, 3. On the other hand the Latin indices  $a, b, c, d$  are 3-dimensional, with range 1, 2, 3.

## 2. The Poincaré Gauge Theory

In the Poincaré gauge theory of gravity (PGT) [7, 8], the two sets of local gauge potentials are, for “translations”, the orthonormal co-frame  $\vartheta^\alpha = e^\alpha_i dx^i$ , where the metric is  $g = -\vartheta^0 \otimes \vartheta^0 + \delta_{ab} \vartheta^a \otimes \vartheta^b$ , and, for “rotations”, the metric-compatible (Lorentz Lie-algebra valued) connection 1-forms  $\Gamma^{\alpha\beta} = \Gamma^{[\alpha\beta]}_i dx^i$ . The associated field strengths are the torsion and curvature 2-forms

$$T^\alpha := d\vartheta^\alpha + \Gamma^\alpha_\beta \wedge \vartheta^\beta = \frac{1}{2} T^\alpha_{\mu\nu} \vartheta^\mu \wedge \vartheta^\nu, \quad (1)$$

$$R^{\alpha\beta} := d\Gamma^{\alpha\beta} + \Gamma^\alpha_\gamma \wedge \Gamma^{\gamma\beta} = \frac{1}{2} R^{\alpha\beta}_{\mu\nu} \vartheta^\mu \wedge \vartheta^\nu, \quad (2)$$

which satisfy the respective Bianchi identities:

$$DT^\alpha \equiv R^\alpha_\beta \wedge \vartheta^\beta, \quad DR^{\alpha\beta} \equiv 0. \quad (3)$$

The PGT Lagrangian density is taken to have the standard quadratic form; qualitatively,

$$\mathcal{L}[\vartheta, \Gamma] \sim \Lambda - a_0 R + \sum_{n=1}^3 a_n \overset{(n)}{T}^2 + \sum_{n=1}^6 b_n \overset{(n)}{R}^2, \quad (4)$$

where  $\overset{(n)}{T}$  and  $\overset{(n)}{R}$  are the algebraically irreducible parts of the torsion and curvature and  $\Lambda$  is the cosmological constant. The gravitational field equations obtained from varying with respect to the respective gauge potentials  $\vartheta^\alpha_i, \Gamma^{\alpha\beta}_j$  have the qualitative form

$$\Lambda - a_0 G_\alpha^i + \sum_{n=1}^3 a_n (D\overset{(n)}{T} + \overset{(n)}{T}^2) + \sum_{n=1}^6 b_n \overset{(n)}{R}^2 \sim \text{source energy-momentum density}, \quad (5)$$

$$a_0 T + \sum_{n=1}^3 a_n \overset{(n)}{T} + \sum_{n=1}^6 b_n D\overset{(n)}{R} \sim \text{source spin density}. \quad (6)$$

These are, respectively, second order equations<sup>‡</sup> for  $\vartheta^\alpha_i$  and  $\Gamma^{\alpha\beta}_j$ . In conjunction with the Bianchi identities (3), these two equations yield, respectively, the conservation of source energy-momentum and angular momentum statements.

Here, generalizing an earlier work [2], we wish to examine the dynamics of the special case describing the two good PGT dynamic scalar modes in a cosmological model. For this two spin-0 modes case we should take  $b_n = 0$  except for  $b_6 \rightarrow b^+$  and  $b_3 \rightarrow -b^-$  (see Appendix A). For more convenient signs we also make the replacement  $a_n \rightarrow -A_n$ .

The gravitational Lagrangian of our model has the specific form

$$\mathcal{L}[\vartheta, \Gamma] = \frac{1}{2\kappa} \left[ -2\Lambda + A_0 R - \frac{1}{2} \sum_{n=1}^3 A_n \overset{(n)}{T}^2 + \frac{b^+}{12} R^2 + \frac{b^-}{12} E^2 \right], \quad (7)$$

<sup>‡</sup> It should be noted that the PGT is obtained from an action containing quadratic curvature terms, but with the connection as a variable they yield 2nd order equations. Higher order equations *would* result from such an action *if* one used the Christoffel connection—or decomposed the Lorentz connection into a Christoffel part plus torsion terms and then treated the torsion and the metric as the fundamental dynamical fields. Such a decomposition is alien to gauge principles.

where  $\kappa = 8\pi G$ ,  $R$  is the scalar curvature and  $E$  is the pseudoscalar curvature (specifically  $E/6 = R_{[0123]}$  is the magnitude of the one component of the totally antisymmetric curvature). The cosmological constant has been included both for generality and a comparison with other models.

In detail, the first field equation, obtained from variation with respect to the orthonormal frame, has the components

$$\begin{aligned} \Lambda g_{\mu\nu} + A_0 G_{\mu\nu} + A_1 \left( \nabla_\alpha T_{\nu\mu}{}^\alpha + \frac{1}{2} T_{\nu\alpha\beta} T_\mu{}^{\alpha\beta} - T_{\nu\mu\alpha} T^\alpha + \frac{1}{4} g_{\mu\nu} T^{\alpha\beta\gamma} T_{\alpha\beta\gamma} - T_{\alpha\beta\mu} T^{\alpha\beta}{}_\nu \right) \\ + \frac{A_2 - A_1}{3} \left( g_{\mu\nu} \nabla_\alpha T^\alpha - \nabla_\nu T_\mu - \frac{1}{2} g_{\mu\nu} T_\alpha T^\alpha \right) + \frac{A_3 - A_1}{18} (6 \nabla_\alpha P^\beta \epsilon^\alpha{}_{\beta\nu\mu} - 4 P_\alpha T_{\nu\beta\gamma} \epsilon^{\beta\gamma\alpha}{}_\mu \\ + 3 P_\alpha T^\alpha{}_{\beta\gamma} \epsilon^{\beta\gamma}{}_{\nu\mu} - 4 T^\alpha{}_{\beta\nu} P^\gamma \epsilon_\alpha{}^\beta{}_{\gamma\mu} - P_\alpha P^\alpha g_{\mu\nu} + 2 P_\mu P_\nu) - \frac{b^-}{24} (E^2 g_{\mu\nu} - 2 E R_{\alpha\beta\gamma\nu} \epsilon^{\alpha\beta\gamma}{}_\mu) \\ + \frac{b^+}{24} (4 R_{\mu\nu} - R g_{\mu\nu}) R = \kappa \mathcal{T}_{\mu\nu} \end{aligned} \quad (8)$$

where  $G_{\mu\nu} = R_{\mu\nu} - \frac{1}{2} g_{\mu\nu} R$  is the Einstein tensor and  $\mathcal{T}_{\mu\nu}$  is the (in general nonsymmetric) material energy-momentum density tensor.

The components of the second field equation, obtained from the variation with respect to the connection, can be decomposed into three algebraically irreducible parts:

$$(6(A_0 - A_1) + b^+ R) T^{\alpha}{}_{\beta\gamma}{}^{(1)} - \frac{b^-}{2} E T^{\alpha}{}_{\mu\nu} \epsilon^{\mu\nu}{}_{\beta\gamma}{}^{(1)} = 0, \quad (9)$$

$$b^+ \nabla_\mu R - \frac{2}{3} (6m^+ + b^+ R) T_\mu + \frac{1}{3} b^- E P_\mu = 0, \quad (10)$$

$$b^- \nabla_\mu E - \frac{1}{3} (6m^- + b^+ R) P_\mu - \frac{2}{3} b^- E T_\mu = \kappa S_\mu = 0, \quad (11)$$

where  $T_\mu \equiv T^\alpha{}_{\alpha\mu} = T^{\alpha}{}_{\alpha\mu}{}^{(2)}$ ,  $P_\mu \equiv \frac{1}{2} \epsilon_{\mu\nu}{}^{\alpha\beta} T^\nu{}_{\alpha\beta} = \frac{1}{2} \epsilon_{\mu\nu}{}^{\alpha\beta} T^{\nu}{}_{\alpha\beta}{}^{(3)}$  are the torsion trace and axial vectors,  $m^+ \equiv A_0 + A_2/2$  and  $m^- \equiv A_0 + 2A_3$  are the masses of the respective linearized modes, and  $S_\mu$  is the axial vector spin density which, for simplicity, we have assumed to vanish (this should be a good approximation except at high densities such as those expected in the very early universe). The  $0^-$  part couples, as indicated here, to the axial spin vector of spin-1/2 fermions, but the  $0^+$  mode *does not couple to any known source*.

From (9) we find the general solution  $T^{\alpha}{}_{\beta\gamma}{}^{(1)} = 0$ . From (10) and (11) we learn that the torsion trace and axial vectors are controlled by the gradients of two functions. This reflects their respective spin  $0^+$ , spin  $0^-$  fundamental nature. However, in view of the non-linearities of these relations as well as the geometric significance of the respective ‘‘potential functions’’ (i.e., they are the scalar and pseudoscalar curvatures), one can see that it is neither possible nor appropriate to resolve them to find new, simpler dynamics for two ‘‘scalar potentials’’.

### 3. The PGT scalar mode cosmological model

For a homogeneous, isotropic FLRW (Friedmann-Lemaître-Robinson-Walker) cosmological model the isotropic orthonormal coframe has the form

$$\vartheta^0 = dt, \quad \vartheta^a = a(t) \left(1 + \frac{1}{4}kr^2\right)^{-1} dx^a, \quad (12)$$

where  $k = -1, 0, +1$  is the sign of the Riemannian spatial curvature. Here we will consider for simplicity only the flat  $k = 0$  case (as far as the observations can tell, this appears to well describe our physical universe).

Because of isotropy, for this  $k = 0$  case the only non-vanishing connection one-form coefficients are of the form

$$\Gamma^a_0 = \Psi(t) dx^a, \quad \Gamma^a_b = X(t) \epsilon^a_{bc} dx^c, \quad (13)$$

where  $\epsilon_{abc} := \epsilon_{0abc}$  is the usual 3 dimensional Levi-Civita anti-symmetric tensor. From the definition of the curvature (2), one can now find all the nonvanishing curvature 2-forms:

$$R^{0a} = \dot{\Psi} dt \wedge dx^a - X \Psi \epsilon^a_{bc} dx^b \wedge dx^c, \quad R^{ab} = \dot{X} \epsilon^{ab}_c dt \wedge dx^c + (\Psi^2 - X^2) dx^a \wedge dx^b. \quad (14)$$

Consequently, the scalar and pseudoscalar curvatures are, respectively,

$$R = 6[a^{-1}\dot{\Psi} + a^{-2}(\Psi^2 - X^2)], \quad (15)$$

$$E = 6[a^{-1}\dot{X} + 2a^{-2}X\Psi]. \quad (16)$$

Because of isotropy, the only nonvanishing torsion tensor components are of the form

$$T^a_{b0} = f(t) \delta^a_b, \quad T^a_{bc} = -2\chi(t) \epsilon^a_{bc}. \quad (17)$$

From the definition of the torsion (1) one can find the relation between the torsion components and the gauge variables:

$$f = a^{-1}(\Psi - \dot{a}), \quad \chi = a^{-1}X. \quad (18)$$

(Note: the variable  $\Phi = -3f$  was used in the earlier work [2].)

From the isotropic assumption, the material energy momentum tensor must have the perfect fluid form. In this work we focus on the late time behavior. Accordingly we assume that the fluid pressure can be neglected, so that the gravitating material behaves like dust with a density satisfying  $\rho a^3 = \text{constant}$ . Also, we remind the reader that, although we expect the spin density to play an important role in the early universe, it is reasonable to assume that the material spin density is negligible at late times.

Due to isotropy, the first field equation (8) has only two nontrivial distinct components. Expressed in terms of the tensorial quantities and the Hubble parameter  $H = \dot{a}/a$  they are the “00” piece

$$\begin{aligned} &+ \Lambda + \frac{3A_2}{2} H^2 - 3m^+(H + f)^2 + 3m^-\chi^2 \\ &+ \frac{b^-}{24} E^2 - b^- E(H + f)\chi + \frac{b^+}{24} R^2 - \frac{b^+}{2} R[(H + f)^2 - \chi^2] = -\kappa\rho, \end{aligned} \quad (19)$$

which contains only first time derivatives of the potentials (and is hence an initial value constraint), and the “space-space” piece

$$\begin{aligned}
& -\Lambda + \frac{m^+}{3}[R - 3(H + f)^2] + (2m^+ - m^-)\chi^2 - \frac{A_2}{2}(2\dot{H} + 3H^2) \\
& + \frac{b^-}{72}E^2 - \frac{b^-}{3}E(H + f)\chi + \frac{b^+}{72}R^2 - \frac{b^+}{6}R[(H + f)^2 - \chi^2] = -\kappa p = 0, \tag{20}
\end{aligned}$$

a dynamical equation for  $\ddot{a}$ .

From the components of the second field equation (10,11), we obtain

$$b^+ \dot{R} = 2(b^+ R + 6m^+)f + 2b^- E\chi, \tag{21}$$

$$b^- \dot{E} = 2b^- E f - 2(b^+ R + 6m^-)\chi, \tag{22}$$

which—along with the definition of the curvature scalars (15), (16) — are second order dynamical equations for the connection coefficients.

Before we present our more detailed discussion of these dynamical equations it should be noted that there are some special “non-dynamic effective cosmological constant” cases—that is special cases having one constant magnitude field when certain coefficients a/o other field components vanish. Such field components would contribute to the dynamical equations certain constant terms that would act like effective cosmological constants. Since here we are interested in the generic case with both modes dynamic, we only mention these special cases briefly and cite other works where they have been considered in more detail. In particular [2] discussed the case with vanishing  $b^-$ ,  $\chi$  and  $R = -6m^+/b^+$ , while [32] has considered the case with vanishing  $b^-$ ,  $f$ , and  $R = -6m^-/b^+$ . It should also be mentioned that the earlier investigators have tended to decompose the connection into its Christoffel part plus some torsion. Using such a decomposition leads to higher order equations—unless one takes  $A_2 = 0$ , as these investigators were prone to do (see, e.g., [28, 29, 30, 32, 33]. Here *we do not make such a decomposition of the connection* and need not make such a parameter restriction—which would in fact render the  $0^+$  mode non-dynamic.

Instead of considering the three second-order differential equations (20,21,22,), we can transform these second-order equations into six first-order differential equations by including the definition of  $H$  and (15)–(16) for the six unknown variables:  $a$ ,  $H$ ,  $f$ ,  $\chi$ ,  $R$ , and  $E$  (where all except  $a$  and  $H$  are gauge covariant tensor fields). For some purposes this is more convenient; in particular first-order differential equations are more suitable for numerical calculations. Combining Eqs. (19) and (20) gives

$$-3A_2(\dot{H} + 2H^2) + m^+ R - 4\Lambda + 6(m^+ - m^-)\chi^2 = \kappa(\rho - 3p) = \kappa\rho. \tag{23}$$

Eq. (23) is considered as a first-order differential equation for  $H$ . Moreover, Eqs. (21) and (22) are already first-order differential equations for  $R$  and  $E$ . After replacing  $\dot{H}$  in Eq. (15) by using (23), it is clear that Eqs. (15) and (16) give the first-order equations for  $f$  and  $\chi$ . With a straightforward re-organization, the six equations are

$$\dot{a} = aH, \tag{24}$$

$$\dot{H} = \frac{m^+}{3A_2}R + \frac{2(m^+ - m^-)}{A_2}\chi^2 - 2H^2 - \frac{\kappa\rho}{3A_2} - \frac{4\Lambda}{3A_2}, \tag{25}$$



$$\dot{f} = \frac{4A_3}{A_2}\chi^2 - \frac{A_0}{3A_2}R - f^2 - 3Hf + \frac{\kappa\rho}{3A_2} + \frac{4\Lambda}{3A_2}, \quad (26)$$

$$\dot{\chi} = \frac{E}{6} - (3H + 2f)\chi, \quad (27)$$

$$\dot{R} = \frac{2b^-}{b^+}\chi E + 2f\left(R + \frac{6m^+}{b^+}\right), \quad (28)$$

$$\dot{E} = 2fE - \frac{2b^+}{b^-}\chi\left(R + \frac{6m^-}{b^+}\right), \quad (29)$$

with the constraint equation

$$\Lambda + \frac{3}{2}A_2H^2 + 3m^-\chi^2 - 3m^+(f+H)^2 + \frac{b^+}{24}R^2 + \frac{b^-}{24}E^2 - b^-E(f+H)\chi - \frac{b^+}{2}R[(f+H)^2 - \chi^2] = -\kappa\rho. \quad (30)$$

The constraint equation can be used to replace  $\kappa\rho$  in Eqs. (25,26) to give alternative versions of these two equations:

$$\begin{aligned} \dot{H} = & -\frac{1}{A_2}\Lambda + \frac{m^+}{3A_2}R - \frac{3}{2}H^2 + \frac{2m^+ - m^-}{A_2}\chi^2 - \frac{m^+}{A_2}(f+H)^2 \\ & + \frac{1}{3A_2}\left\{\frac{b^+}{24}R^2 - \frac{b^+}{2}R[(f+H)^2 - \chi^2] + \frac{b^-}{24}E^2 - b^-E(f+H)\chi\right\}, \end{aligned} \quad (31)$$

$$\begin{aligned} \dot{f} = & \frac{1}{A_2}\Lambda - \frac{A_0}{3A_2}R - \frac{1}{2}f^2 - 2Hf + \frac{2A_3}{A_2}\chi^2 + \frac{A_0}{A_2}[(f+H)^2 - \chi^2] \\ & - \frac{1}{3A_2}\left\{\frac{b^+}{24}R^2 - \frac{b^+}{2}R[(f+H)^2 - \chi^2] + \frac{b^-}{24}E^2 - b^-E(f+H)\chi\right\}. \end{aligned} \quad (32)$$

These two alternative equations along with the four other first order equations make a closed system for the geometric variables which is more practical for numerical evolution. This alternative system will be obtained in another way in the next section.

For a comparison with GR models, the “00” constraint (19) can be considered as a generalized Friedman equation:

$$3A_0H^2 = \kappa(\rho + \rho_\Gamma) + \Lambda, \quad (33)$$

where the effective energy due to the dynamic connection is

$$\kappa\rho_\Gamma = 3m^-\chi^2 - 6m^+Hf - 3m^+f^2 + \frac{b^+}{24}R^2 + \frac{b^-}{24}E^2 - b^-E\chi(H+f) - \frac{b^+}{2}R[(H+f)^2 - \chi^2], \quad (34)$$

Moreover, the “space-space” Eq. (20) may be considered as a force-balance equation:

$$A_0\left(\frac{\ddot{a}}{a}\right) = -\frac{\kappa(\rho + 3p)}{6} - \frac{\kappa(\rho_\Gamma + 3p_\Gamma)}{6} + \frac{\Lambda}{3}, \quad (35)$$

where the effective pressure due to the dynamic connection is

$$\begin{aligned} \kappa p_\Gamma = & 2m^+\dot{f} + m^+f(4H+f) - m^-\chi^2 \\ & + \frac{b^+}{72}R^2 + \frac{b^-}{72}E^2 - \frac{b^-}{3}E\chi(H+f) - \frac{b^+}{6}R[(H+f)^2 - \chi^2]. \end{aligned} \quad (36)$$

It can here be seen how  $\rho_\Gamma + 3p_\Gamma < 0$ , which is indeed possible, could produce an accelerated universe. Although these relations are useful for comparison with other models, an

examination of the dynamical terms implicit in  $\rho_\Gamma$  and  $p_\Gamma$  shows that their PGT dynamic nature differs fundamentally from that of their GR counterparts. In particular the ratio  $w_\Gamma := P_\Gamma/\rho_\Gamma$  can take on any value and should not be given the usual equation-of-state interpretation.

#### 4. Effective Lagrangian and Hamiltonian

Our cosmological model system of ODEs resemble those of a particle with three degrees of freedom. One may suspect that they can be obtained directly from a variational principle. To achieve such a goal it is natural to consider imposing the homogeneous-isotropic symmetry into the field theory Lagrangian density. We note that it has long been known that imposing symmetries and variations do not commute in general. However, for GR they are known to commute for all Bianchi class A cosmologies [37]. We conjecture that this is also true for the PGT. In particular our  $k = 0$  model is an isotropic Bianchi I (class A) model, so there is good reason to be hopeful. Here we show that (at least for our dust fluid model) imposing the FLRW symmetry on the PGT Lagrangian does indeed lead us to the same expressions as were found from imposing the symmetry on the field equations.

Imposing the FLRW symmetry on the Lagrangian density (7) leads to the effective Lagrangian

$$L_{\text{eff}} = \frac{a^3}{\kappa} \left[ -\Lambda + \frac{A_0}{2}R + \frac{3}{2}A_2f^2 - 6A_3\chi^2 + \frac{b^+}{24}R^2 + \frac{b^-}{24}E^2 \right]. \quad (37)$$

It should be noted that (for least action) the coefficients of the quadratic kinetic terms ( $f^2$ ,  $R^2$ ,  $E^2$ ) which contain the time derivatives—see the specific expressions for the curvature and torsion Eqs. (15,16,18)—must be non-negative.

Now we use this effective Lagrangian (along with the just mentioned expressions for the curvature and torsion) to obtain a conserved energy and three second order equations for the gauge parameters: the connection coefficients  $\psi$ ,  $X$  and the frame/metric scale factor  $a$ . We also note that the second order Lagrange equations can be rearranged and combined with the formulas for curvature and torsion to give exactly the six first order equations obtained from the general 4D covariant field equations specialized to the  $k = 0$  FLRW geometry. Following this we will then find the associated Hamiltonian equations.

Making use of the formulas for the torsion and curvature components in terms of the gauge variables, (15,16,18), the conserved energy function associated with  $L_{\text{eff}}$  is found to be

$$\mathcal{E} := \dot{q}^k \frac{\partial L_{\text{eff}}}{\partial \dot{q}^k} - L_{\text{eff}} = \frac{a^3}{\kappa} \left\{ \Lambda + \frac{3A_2}{2}H^2 - 3m^+(f + H)^2 + 3m^-\chi^2 + \frac{b^-}{24}E^2 - b^-E(H + f)\chi + \frac{b^+}{24}R^2 - \frac{b^+}{2}R[(H + f)^2 - \chi^2] \right\}, \quad (38)$$

where  $q_k = \{\Psi, X, a\}$ . This is a combination that we recognize from our earlier analysis, it is just the “00 constraint” (30); its constant magnitude is the physical combination  $-a^3\rho$ , which is indeed a constant because of the dust fluid energy-momentum conservation relation.

Making use of the formulas for the torsion and curvature components in terms of the gauge variables (15,16,18) we now obtain the Euler-Lagrange equations

$$\frac{d}{dt} \frac{\partial L_{\text{eff}}}{\partial \dot{q}_i} - \frac{\partial L_{\text{eff}}}{\partial q_i} = 0.$$

For the  $\Psi$  equation:

$$\frac{d}{dt} \frac{\partial L_{\text{eff}}}{\partial \dot{\Psi}} = \frac{d}{dt} \left( 3A_0 a^2 + \frac{b^+}{2} a^2 R \right) = \frac{\partial L_{\text{eff}}}{\partial \Psi} = 6A_0 a \Psi + b^+ a R \Psi + b^- a E X + 3A_2 a^2 f. \quad (39)$$

This is a second order equation for  $\Psi$ . (Here and below we dropped for simplicity the overall factor of  $\kappa^{-1}$ .) It can alternately be rearranged using (18) to give (28), the first order equation for  $\dot{R}$ .

For the  $X$  equation:

$$\frac{d}{dt} \frac{\partial L_{\text{eff}}}{\partial \dot{X}} = \frac{d}{dt} \left( \frac{1}{2} b^- a^2 E \right) = \frac{\partial L_{\text{eff}}}{\partial X} = b^- a E \Psi - b^+ a X R - 6A_0 a X - 12A_3 a X. \quad (40)$$

This second order equation for  $X$  can be rearranged using (18) into (29), the first order equation for  $\dot{E}$ .

For the  $a$  equation:

$$\begin{aligned} \frac{d}{dt} \frac{\partial L_{\text{eff}}}{\partial \dot{a}} = \frac{d}{dt} (-3A_2 a^2 f) = \frac{\partial L_{\text{eff}}}{\partial a} = & A_0 [a^2 R - 3(\Psi^2 - X^2)] + \frac{b^+}{24} a^2 R^2 - \frac{b^+}{2} R(\Psi^2 - X^2) \\ & + \frac{b^-}{24} a^2 E^2 - b^- X \Psi E + \frac{3}{2} A_2 a^2 f^2 - 6A_3 X^2 - 3\Lambda a^2. \end{aligned} \quad (41)$$

This is a second order equation for  $a$ . It can be rearranged into a first order equation for  $\dot{f}$ ; the result is exactly (32), the aforementioned alternative to (26) obtained by using (30). Now using (18) one can calculate

$$\dot{H} = \frac{d}{dt} (a^{-1} \Psi) - \dot{f} = -H(H + f) + a^{-1} \dot{\Psi} - \dot{f}, \quad (42)$$

then using the just mentioned expression for  $\dot{f}$  and (15) one gets (31). Moreover, from (16) using (18) one gets the  $\dot{\chi}$  equation (27).

It is remarkable that here in these Lagrange equations and the associated conserved energy we get (at least for this dust case) exactly the correct equations for our model—*without including any explicit source coupling!*

We have cast our system into six first order equations for (3D) tensorial quantities, equations which are suitable for numeric evolution and comparison with observations. However these equations are probably not in the most suitable form for the most penetrating analytic analysis. So we here also present the Hamiltonian equations for our PGT cosmology.

From the above one can introduce the canonical conjugate momentum variables:

$$P_a \equiv \frac{\partial L_{\text{eff}}}{\partial \dot{a}} = -\frac{3A_2}{\kappa} a^2 f, \quad (43)$$

$$P_\Psi \equiv \frac{\partial L_{\text{eff}}}{\partial \dot{\Psi}} = a^2 \left( \frac{3A_0}{\kappa} + \frac{b^+}{2\kappa} R \right), \quad (44)$$

$$P_X \equiv \frac{\partial L_{\text{eff}}}{\partial \dot{X}} = \frac{b^-}{2\kappa} a^2 E. \quad (45)$$

Now one can construct the effective Hamiltonian:

$$H_{\text{eff}} = P_a \dot{a} + P_\Psi \dot{\Psi} + P_X \dot{X} - L_{\text{eff}} = \frac{\kappa}{6a} \left( \frac{P_a^2}{A_2} + \frac{P_X^2}{b^-} + \frac{P_\Psi^2}{b^+} \right) - \left( \frac{A_0 a^2}{b^+} + \Psi^2 - X^2 \right) \frac{P_\Psi}{a}$$

$$+ \Psi P_a - \frac{2}{a} X \Psi P_X + \frac{6A_3}{\kappa} a X^2 + \left[ \frac{3A_0^2}{2b^+} + \Lambda \right] \frac{a^3}{\kappa}, \quad (46)$$

and obtain the six Hamilton equations:

$$\dot{a} = \frac{\partial H_{\text{eff}}}{\partial P_a} = \frac{\kappa P_a}{3A_2 a} + \Psi, \quad (47)$$

$$\dot{\Psi} = \frac{\partial H_{\text{eff}}}{\partial P_\Psi} = \frac{\kappa}{3b^+ a} P_\Psi - \frac{\Psi^2}{a} + \frac{X^2}{a} - \frac{A_0}{b^+} a, \quad (48)$$

$$\dot{X} = \frac{\partial H_{\text{eff}}}{\partial P_X} = \frac{\kappa}{3b^- a} P_X - \frac{2}{a} X \Psi, \quad (49)$$

$$\dot{P}_a = -\frac{\partial H_{\text{eff}}}{\partial a} = \frac{H_{\text{eff}} - \Psi P_a}{a} - \frac{12A_3}{\kappa} X^2 - \left[ \frac{2A_0^2}{b^+} + \Lambda \right] \frac{3a^2}{\kappa} + \frac{2A_0}{b^+} P_\Psi, \quad (50)$$

$$\dot{P}_\Psi = -\frac{\partial H_{\text{eff}}}{\partial \Psi} = -P_a + \frac{2}{a} (\Psi P_\Psi + P_X X), \quad (51)$$

$$\dot{P}_X = -\frac{\partial H_{\text{eff}}}{\partial X} = -\frac{12A_3}{\kappa} a X + \frac{2}{a} (P_X \Psi - P_\Psi X). \quad (52)$$

This canonical reformulation should be of considerable interest for further studies of this model, since the Hamiltonian formulation is the framework for the most powerful known approaches for analytically studying the dynamics of a system, including such techniques as the Hamilton-Jacobi method and phase space portraits.

## 5. Asymptotic Expansion

At late times in an expanding universe as the scale factor  $a$  becomes larger the field amplitudes should be decreasing. We can then expect the quadratic terms in (38) to be dominant; hence, when the cosmological constant vanishes the late time asymptotic behavior of  $H$ ,  $f$ ,  $\chi$ ,  $R$ , and  $E$  should have a  $a^{-3/2}$  fall off. So we reparametrize them according to

$$H = ha^{-3/2}, \quad f = ya^{-3/2}, \quad \chi = xa^{-3/2}, \quad R = ra^{-3/2}, \quad E = ea^{-3/2}. \quad (53)$$

The current Universe corresponds to  $a^{3/2} \gg 1$ . Substituting (53) into (24)–(30) gives

$$\dot{a} = a^{-1/2} h, \quad (54)$$

$$\dot{h} = a^{-3/2} \left[ \frac{2(m^+ - m^-)}{A_2} x^2 - \frac{h^2}{2} - \frac{\kappa}{3A_2} \rho_0 a^3(0) \right] + \frac{m^+}{3A_2} r - a^{3/2} \frac{4\Lambda}{3A_2}, \quad (55)$$

$$\dot{y} = a^{-3/2} \left[ \frac{4A_3}{A_2} x^2 - y^2 - \frac{3}{2} h y + \frac{\kappa}{3A_2} \rho_0 a^3(0) \right] - \frac{A_0}{3A_2} r + a^{3/2} \frac{4\Lambda}{3A_2}, \quad (56)$$

$$\dot{r} = a^{-3/2} \left[ 2yr + \frac{3}{2} r h + \frac{2b^-}{b^+} e x \right] + \frac{12m^+}{b^+} y, \quad (57)$$

$$\dot{x} = a^{-3/2} \left[ -2xy - \frac{3}{2} h x \right] + \frac{e}{6}, \quad (58)$$

$$\dot{e} = a^{-3/2} \left[ 2ey + \frac{3}{2} h e - \frac{2b^+}{b^-} r x \right] - \frac{12m^-}{b^-} x, \quad (59)$$

$$-a^3 \kappa \rho = -\kappa \rho_0 a^3(0) = a^3 \Lambda + \frac{3A_2}{2} h^2 + 3m^- x^2 + \frac{b^-}{24} e^2 + \frac{b^+}{24} r^2 - 3m^+ (y + h)^2$$

$$- a^{-3/2} \left[ b^- e x (h + y) + \frac{b^+}{2} r ((h + y)^2 - x^2) \right]. \quad (60)$$

Now let us restrict our further considerations to the vanishing cosmological constant case. With  $a^{3/2} \gg 1$ , Eqs. (54)–(59) show that the spin-0<sup>+</sup> mode and the spin-0<sup>-</sup> mode are becoming decoupled and the asymptotic Hubble rate  $h$  is influenced purely by the spin-0<sup>+</sup> mode. Dropping the higher order terms (with  $\Lambda = 0$ ), gives the energy constraint

$$- a^3 \kappa \rho = -\kappa \rho_0 a^3(0) = \frac{3A_2}{2} h^2 + 3m^- x^2 + \frac{b^-}{24} e^2 + \frac{b^+}{24} r^2 - 3m^+ (y + h)^2 \quad (61)$$

and three natural pairs of linear equations:

$$(\dot{a} = a^{-1/2} h, \quad \dot{h} = \frac{m^+}{3A_2} r), \quad (\dot{y} = -\frac{A_0}{3A_2} r, \quad \dot{r} = \frac{12m^+}{b^+} y), \quad (\dot{x} = \frac{e}{6}, \quad \dot{e} = -\frac{12m^-}{b^-} x). \quad (62)$$

The last two pairs,  $(y, r)$  and  $(x, e)$ , are clearly harmonic oscillators. To analyze these equations further along with the first pair, we introduce the new variable combination

$$z := m^+ y + A_0 h. \quad (63)$$

We then find three late time normal modes:

$$\ddot{x} + \omega_-^2 x = 0, \quad \text{where} \quad \omega_-^2 = \frac{2m^-}{b^-} \quad (64)$$

$$\ddot{y} + \omega_+^2 y = 0, \quad \text{where} \quad \omega_+^2 = \frac{4A_0 m^+}{A_2 b^+} \quad (65)$$

$$\dot{z} = 0. \quad (66)$$

Reexpressed in terms of the late time normal modes the late-time energy constraint is

$$\text{const.} = -a^3 \kappa \rho = -\frac{3}{A_0} z^2 + \left( \frac{3A_2}{2A_0} m^+ y^2 + \frac{b^+}{24} r^2 \right) + \left( 3m^- x^2 + \frac{b^-}{24} e^2 \right), \quad (67)$$

where each bracket is constant. The physical and geometric significance of two of the normal modes is clear, since they directly correspond to the two torsion magnitudes (alternately the associated curvature scalars). Thus for this model at late time we find that the two *dynamical connection* modes are essentially *dynamical torsion modes* and the description “torsion cosmology” is phenomenologically appropriate, although it could lead to a misapprehension as to the true fundamental dynamical fields.§

The remaining mode  $z$  corresponds to a certain combination of the frame/metric scale expansion factor and the 0<sup>+</sup> torsion:

$$Z = m^+ f + A_0 H \quad (68)$$

which evolves according to

$$\dot{Z} = m^- \chi^2 - m^+ f (f + 3H) - 2A_0 H^2 + \frac{\kappa \rho}{6}. \quad (69)$$

§ Although the terminology “torsion cosmology” has often been used in the past to describe the sort of model we are considering here, it has recently come to our attention that such terms are fundamentally inappropriate and can inhibit a deeper understanding. The basic dynamic variables in this theory are the orthonormal frame and connection.

(With a nonvanishing cosmological constant this equation would pick up an extra  $2\Lambda/3$  term.) From the above we see that at late time (with vanishing cosmological constant) the Hubble expansion rate has the form

$$H = a^{-3/2} \times \text{const.} - \frac{m^+}{A_0} f, \quad (70)$$

with the  $0^+$  torsion amplitude  $f$  oscillating at the frequency  $\omega_+$ . Only the  $0^+$  mode effects the expansion rate at late times. The late time acceleration is

$$\ddot{a} = a^{-1/2} \frac{m^+}{3A_2} r, \quad (71)$$

which has periodic oscillations at the rate  $\omega_+$ . In this model sometimes the expansion rate is accelerating and sometimes it is slowing down.

### 5.1. Numerical test

The validity of our late time analytic results has been tested numerically. Taking the parameters as  $A_0 = 1$ ,  $A_2 = 0.23$ ,  $A_3 = -0.35$ ,  $b^+ = 1.1$ , and  $b^- = 0.3$ , we find  $\omega_+ = 4.20$  and  $\omega_- = 1.4$ . They have the relation  $\omega_+ = 3\omega_-$ . Using the same parameters, we plot a full and a linear asymptotic normal mode evolution of all the 6 dynamical equations. The behavior of the normal mode equations has been observed with several sets of initial values.

We have plotted one typical case in Fig. 1. Here we show at late time the asymptotic amplitudes: first, the Hubble function,  $h$ , second, the normal mode combination of the torsion and Hubble function,  $z$ , third, the spin- $0^-$  normal mode,  $x$ , fourth, the spin- $0^+$  normal mode,  $y$ . The (black) dashed lines represent the exact evolution and the (red) solid lines represent the late time asymptotic normal mode behavior.

As expected, we found that the late time equations are indeed a good approximation. The  $z(t)$  function approaches a flat line at late time. The plots show that the frequency and amplitude of the full and the linear approximation  $0^+$  and  $0^-$  asymptotic equations are very close, although there are apparently still some nonlinear effects.

## 6. Numerical Demonstration

In this section, we present the results of a numerical evolution of our cosmological model. For all these calculations we take  $\Lambda = 0$ . Since there is one scalar mode and one pseudoscalar mode in this model, it is natural to investigate the interaction between these two modes. We find that the pseudoscalar connection mode can generate the scalar connection mode, but not conversely. This offers a reason for the existence of the scalar mode, since it is believed that the pseudoscalar mode exists and plays an important role in the early universe due to its direct interaction with matter. In Section 6.2, we first extend the numerical demonstration of the earlier work [2] by including the spin- $0^-$  mode, and then compare our numerical results with the observational supernovae data. Not surprisingly we find that the supernovae data can be better fitted with the two-scalar-connection-mode model.

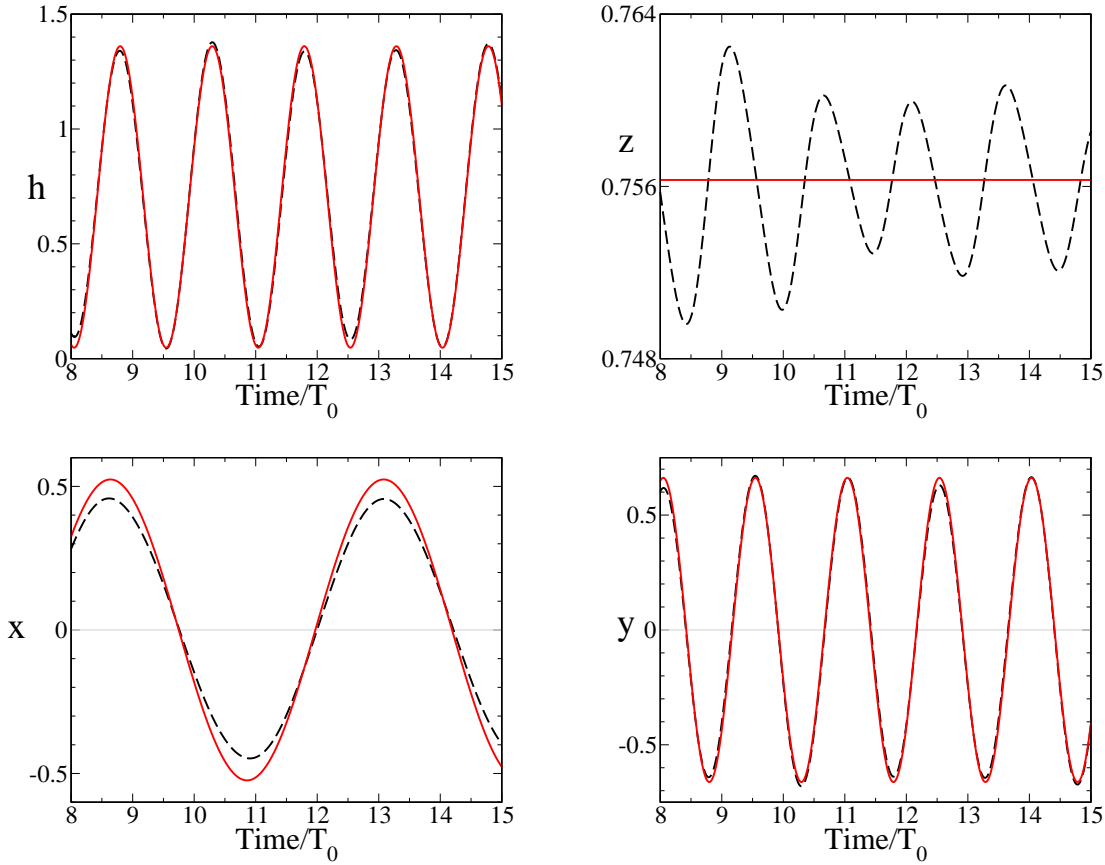


**Figure 1.** Asymptotic evolution of the Hubble function,  $h$ , the late time normal mode combination of torsion and Hubble function,  $z$  (note the scale), the late time spin-0<sup>-</sup> normal mode,  $x$ , and the late time spin-0<sup>+</sup> normal mode,  $y$ . The (black) dashed lines represent the actual late time asymptotic evolution and the (red) solid lines represent the linear approximation normal modes.

We need to look into the scaling features of this model before we can obtain the sort of evolution results we seek on a cosmological scale. In terms of fundamental units we can scale the variables and the parameters as

$$\begin{aligned}
 t &\rightarrow t/\ell, & a &\rightarrow a, & H &\rightarrow \ell H, & f &\rightarrow \ell f, & \chi &\rightarrow \ell \chi, & R &\rightarrow \ell^2 R, & E &\rightarrow \ell^2 E, \\
 A_0 &\rightarrow A_0, & A_2 &\rightarrow A_2, & A_3 &\rightarrow A_3, & b^+ &\rightarrow b^+/\ell^2, & b^- &\rightarrow b^-/\ell^2, & \Lambda &\rightarrow \ell^2 \Lambda,
 \end{aligned} \tag{72}$$

where  $\ell^2 \equiv \kappa = 8\pi G$ . So the variables and the scaled parameters  $b^+$  and  $b^-$  become dimensionless (from the Newtonian limit  $A_0 = 1$ ). Equations. (24–29) remain unchanged under such a scaling. However, as we are interested in the cosmological scale, it is practical to use another scaling—mathematically to make the numerical values of the scaled variables less stiff for the numerical integration, and physically to see changes on the scale of the age of our Universe. In order to achieve this goal, let us introduce a dimensionless constant  $T_0$ , which represents the magnitude of the Hubble time ( $T_0 = H_0^{-1} \doteq 4.41504 \times 10^{17}$  seconds). Then the scaling is

$$t \rightarrow T_0 t, \quad a \rightarrow a, \quad H \rightarrow H/T_0, \quad f \rightarrow f/T_0, \quad \chi \rightarrow \chi/T_0, \quad R \rightarrow R/T_0^2, \quad E \rightarrow E/T_0^2,$$

$$A_0 \rightarrow A_0, \quad A_2 \rightarrow A_2, \quad A_3 \rightarrow A_3, \quad b^+ \rightarrow T_0^2 b^+, \quad b^- \rightarrow T_0^2 b^-, \quad \Lambda \rightarrow \Lambda/T_0^2. \quad (73)$$

With this scaling, all the field equations are kept unchanged while the period  $T \rightarrow T_0 T$ .

### 6.1. The interaction between the scalar and pseudoscalar mode

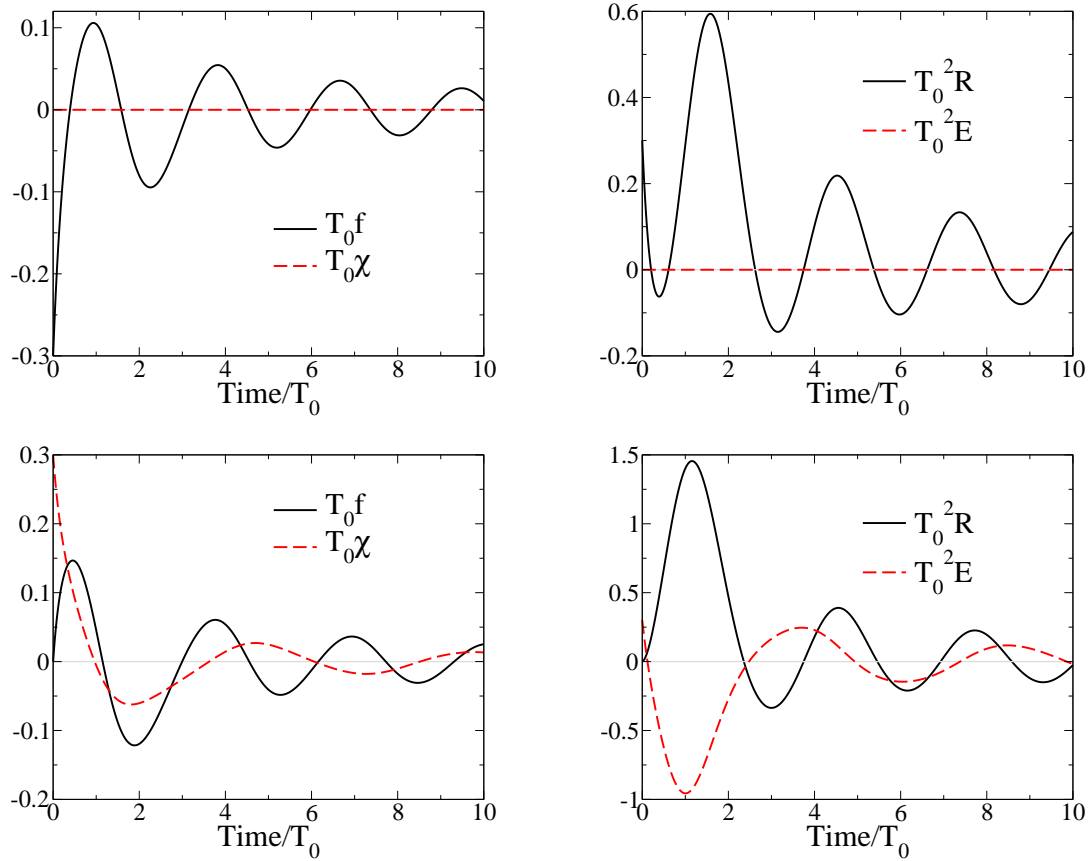


**Figure 2.** Evolution of the components of the torsion. The top panels show the evolution for nonvanishing  $f$  and  $R$ , and vanishing  $\chi$  and  $E$  initially, corresponding to Case (a). The bottom panels show the evolution for nonvanishing  $\chi$  and  $E$ , and vanishing  $f$  and  $R$  initially, corresponding to Case (b).

To understand the interaction of these two propagating scalar connection modes, we consider two different situations: (a) the pseudoscalar mode vanishes initially with a non-vanishing scalar mode; (b) the scalar mode vanishes initially with a non-vanishing pseudoscalar mode. The parameters and the initial values for Case (a) are set as

$$A_2 = 0.5, \quad A_3 = 1, \quad b^+ = 2, \quad b^- = 1, \quad (74)$$

and

$$f(0) = -0.3, \quad R(0) = 0.3, \quad \chi(0) = 0, \quad E(0) = 0, \quad (75)$$

where  $a(0) = 50$  and  $H(0) = 1$  in both the cases. The parameters and the initial values for Case (b) were chosen as

$$A_2 = 1.0, \quad A_3 = -0.1, \quad b^+ = 1.5, \quad b^- = 1, \quad (76)$$



and

$$f(0) = 0, \quad R(0) = 0, \quad \chi(0) = 0.3, \quad E(0) = 0.3. \quad (77)$$

The numerically calculated evolution of these two cases are shown in Fig. 2. Case (a), which corresponds to the top two panels of Fig. 2, shows that the scalar mode cannot generate an initially vanishing pseudoscalar mode. It is clear that  $\chi$  and  $E$  stay zero with a dynamic spin-0<sup>+</sup> mode. The two bottom panels of Fig. 2, which correspond to case (b), show that the pseudoscalar mode can generate an initially vanishing scalar mode. It is known that the pseudoscalar connection mode will couple to elementary spinning particles. One can expect that this mode will be excited by spinning particles in the early Universe, since there could be a high spin density during this epoch. Once the pseudoscalar connection mode is generated, the scalar connection mode will be excited through the interaction with the pseudoscalar connection mode.

## 6.2. Accelerating universes

We would like to compare the numerical evolution values for this model (with  $\Lambda = 0$ ) with the observational data of our Universe. The Hubble constant at present,  $H(t_0 = 1)$ , is

$$H = \frac{1}{4.41504 \times 10^{17}} \cdot \frac{1}{\text{s}} \approx 70 \frac{\text{km}}{\text{s} \cdot \text{Mpc}}. \quad (78)$$

The initial data is set at the current time  $t_0 = 1$ , and current value of the Hubble function is scaled to unity in this work, just as in [2]. The parameters and initial conditions chosen for our first case are as follows:

$$A_2 = 0.83, \quad A_3 = -0.35, \quad b^+ = 1.1, \quad b^- = 0.091, \quad (79)$$

and

$$\begin{aligned} a(t_0 = 1) &= 50, & H(t_0 = 1) &= 1, & f(t_0 = 1) &= -0.335, \\ \chi(t_0 = 1) &= 0.378, & R(t_0 = 1) &= 2.18, & E(t_0 = 1) &= 2.21. \end{aligned} \quad (80)$$

The results of the evolution with these parameters and initial conditions are plotted in Fig. 3. The expansion factor  $a$  is plotted in the top-left panel. In the top-right panel the Hubble function  $H$  is damped-oscillating at late time. In the bottom-right panel, it is obvious that  $\ddot{a}$  is damped and oscillating during the evolution and is positive at the current time  $t \approx 1$ , which means the expansion of the universe is currently accelerating. The torsion and curvature scalars,  $f(t)$ ,  $\chi(t)$ ,  $R(t)$ , and  $E(t)$ , are also plotted in the middle panels of Fig. 3 to show the correlation of the evolution between these variables. We observe that the frequencies of the pairs  $(\chi, E)$  and  $(f, R)$  are usually different. The behavior is consistent with the analysis in Sec. 5. In order to have a deeper understanding of the settings of this case, the matter density  $\rho$  and the effective mass density of the dynamical connection  $\rho_\Gamma$  are plotted in the bottom-left panel. The value of  $\rho$  is decreasing as the universe is expanding and is always positive with  $\rho a^3 = \text{const}$ , while  $\rho_\Gamma$ , plotted in the same panel, shows a “damped-oscillating” behavior. The damped-oscillating behavior of  $\rho_\Gamma$  simply indicates that the effective energy density  $\rho_\Gamma$  is not positive-definite in general. We also plot the phase diagrams for Case I in Fig. 4 to show that

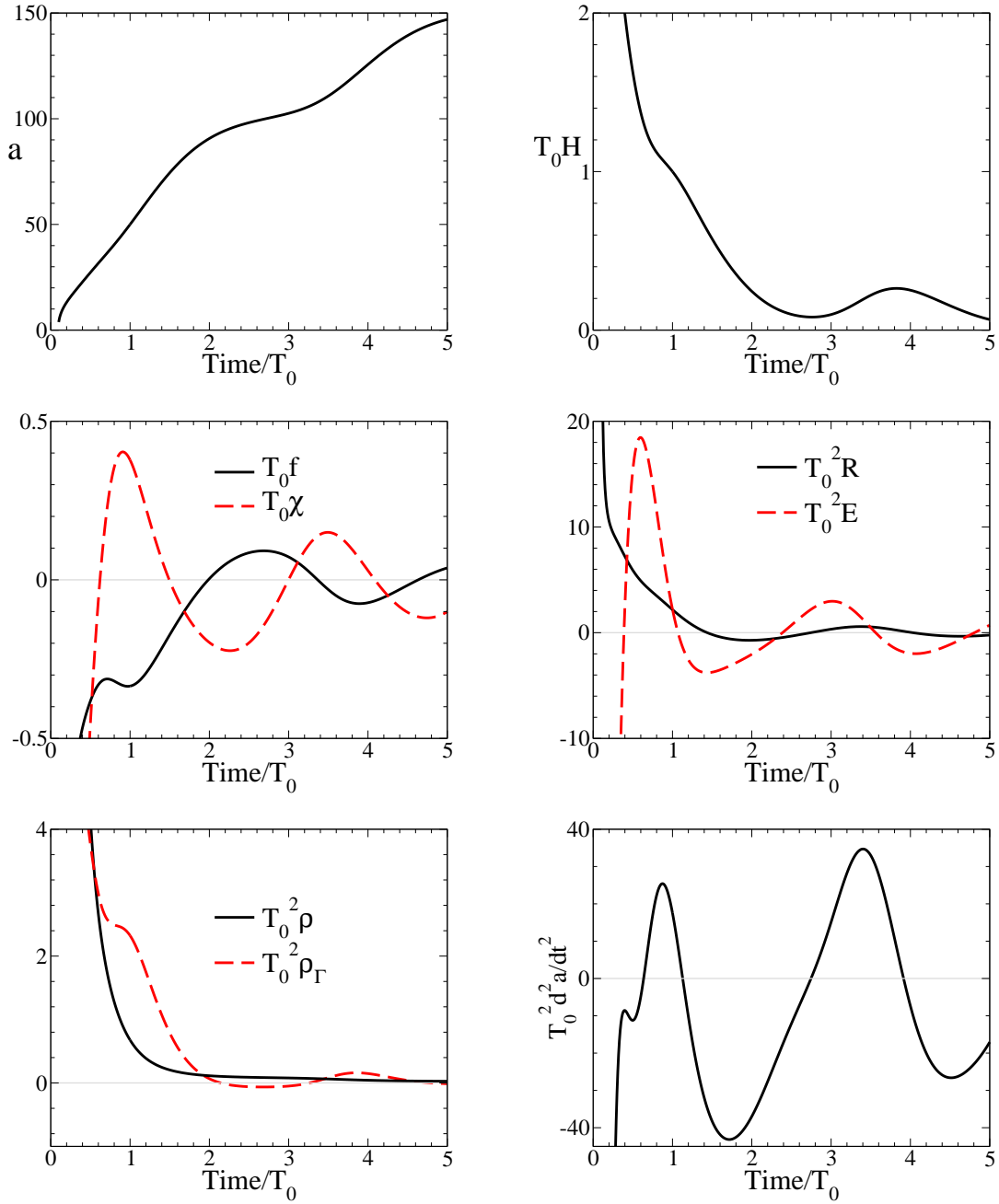


**Figure 3.** Evolution of the expansion factor  $a$ , the Hubble function,  $H$ , the scalar and the pseudoscalar torsion components,  $f$  and  $\chi$ , the affine scalar curvature,  $R$ , the pseudoscalar curvature,  $E$ , the mass densities,  $\rho$  and  $\rho_\Gamma$ , and the 2nd time derivative of the expansion factor,  $\ddot{a}$ , as functions of time with the parameter choice and the initial data in Case I.

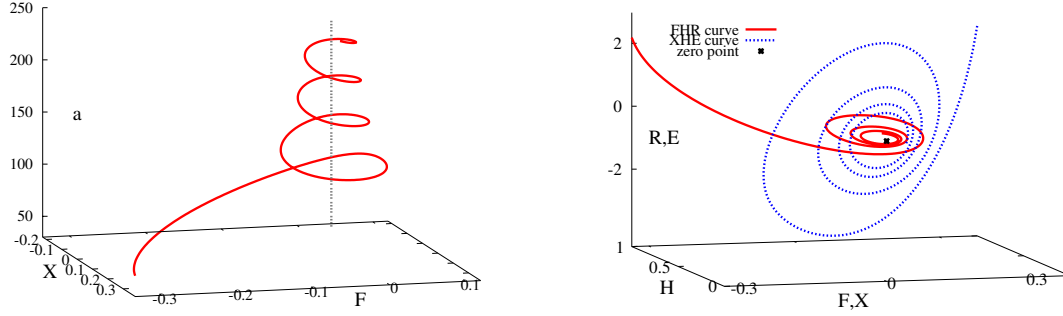


**Figure 4.** The phase diagrams for Case I. The phase diagram of  $(F, \chi, a)$  is shown in the left panel. The (red) solid line is the trajectory of the  $(F, \chi, a)$  evolution starting from the initial value  $(-0.335, 0.378, 50)$ . The (gray) dashed line is the convergence line  $(0, 0, a)$  for this diagram. The phase diagrams of  $(F, H, R)$  and of  $(\chi, H, E)$  are shown in the right panel. The (red) solid line is the trajectory of the  $(F, H, R)$  evolution starting from the initial value  $(-0.335, 1, 2.18)$ , the (blue) dashed line is the trajectory of the  $(\chi, H, E)$  evolution starting from the initial value  $(0.378, 1, 2.21)$ , and the (black) filled point marks the asymptotic focus point  $(0, 0, 0)$ .

**Table 1.** The initial data and parameters for cases I, II, and III. Here the parameter  $A_0 = 1$ ,  $a(t = 1) = 50$ , and  $H(t = 1) = 1$  in all three cases;  $t = 1$  means  $t = \text{now}$ , under the scaling of Eqs. (72–73).

Case	$A_2$	$A_3$	$b^+$	$b^-$	$f(1)$	$\chi(1)$	$R(1)$	$E(1)$	$\Omega_m$
I	0.83	-0.35	1.1	0.091	-0.335	0.378	2.18	2.21	0.23
II	0.52	0.475	1.05	0.35	-0.318	0.225	2.7	-1.2	0.29
III	0.635	0.5	1.06	0.42	-0.361	0.058	2.442	-1.8	0.27

the orbit of  $(f, \chi, a)$  is convergent to a line  $(0, 0, a)$ , and the orbits of  $(f, H, R)$  and of  $(\chi, H, E)$  both converge to the point  $(0, 0, 0)$ .

In this case the scaled value of  $\rho(t = 1) = 0.68$  and its physical value is  $\rho(t = T_0) = 2.15 \times 10^{-30} \text{g/cm}^3$ . The Universe is supposed to be very close to the critical density,  $\rho_c \equiv 3c^2 H^2 / 8\pi G = 9.47 \times 10^{-30} \text{g/cm}^3$ ; we find the ratio  $\Omega_m \equiv \rho / \rho_c \approx 23\%$ . In the standard  $\Lambda$ CDM model,  $\Omega_m \sim 30\%$  with 5% baryonic matter and 25% dark matter. For our model  $\Omega_\Gamma \equiv \rho_\Gamma / \rho_c = 77\%$  acts like the energy density of dark energy. Therefore, this dynamic connection model is able to describe a presently accelerating expansion of the Universe with a proper amount of matter density. From the field equations we can see that the *effect* of the “dark energy” mainly comes from the nonlinearity of the field equation driven by the dynamic scalar and pseudoscalar connection modes. We also found other cases, two of which are listed in Table 1 along with Case I; they are obtained by taking different values for the parameters and the initial conditions. We find that the results for the other two cases have a behavior qualitatively similar to that of Case I.

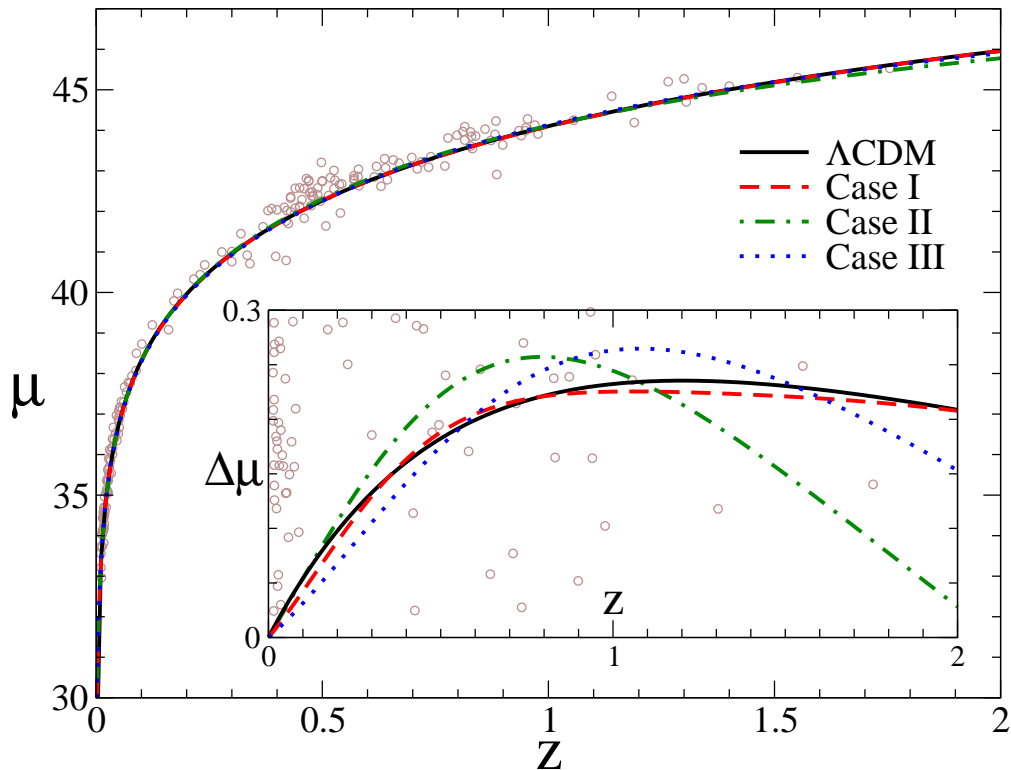


**Figure 5.** Comparison of different spin-zero connection models and the standard  $\Lambda$ CDM model with the observational data via the relation between the distance modulus  $\mu$  and the redshift  $z$ . The supernovae data points, plotted with (brown) circles, come from [38]. The result of the standard  $\Lambda$ CDM model ( $\Omega_m = 0.3$ ,  $\Omega_\Lambda = 0.7$ ) is plotted by the bold solid line. The results of Case I, II, and III are represented by the (red) dashed line, the (green) dot-dashed line, and the (blue) dotted line, respectively. In the inset, the models and data are shown relative to an empty universe model ( $\Omega = 0$ ).

We compare our results with the supernovae data. Distance estimates from SN Ia light curves are derived from the luminosity distance

$$d_L \equiv \sqrt{\frac{L_{\text{int}}}{4\pi\mathcal{F}}} = cT_0 a(1)(1+z) \int_1^t \frac{dt}{a(t)}, \quad (81)$$

where  $L_{\text{int}}$  and  $\mathcal{F}$  are the intrinsic luminosity and observed flux of the SN, and the redshift  $z \equiv a(1)/a(t) - 1$ . Logarithmic measures of the flux (apparent magnitude,  $m$ ) and luminosity (absolute magnitude,  $M$ ) were used to derive the predicted distance modulus

$$\mu = m - M = 5 \log_{10} d_L + 25, \quad (82)$$

where  $m$  is the flux (apparent magnitude),  $M$  is the luminosity (absolute magnitude), and  $d_L$  in the formula should be in units of megaparsecs. We found the relations between the predicted distance modulus  $\mu$  and the redshift  $z$  in the three cases; they are plotted in Fig. 5. For comparison, we also plot the prediction of the  $\Lambda$ CDM model with  $\Omega_m = 0.3$  and  $\Omega_\Lambda = 0.7$

by employing the following formula [38]

$$d_L = cT_0(1+z) \int_0^z \frac{dz}{\sqrt{(1+z)^2(1+\Omega_m z) - z(2+z)\Omega_\Lambda}}. \quad (83)$$

The astronomical observational data [38, 39] are also plotted in Fig. 5 for comparison. The plots show that for small redshift  $z$  (e.g.,  $z < 1.9$ ) all three cases of the dynamical connection models give an accelerating universe just like the  $\Lambda$ CDM model does. For larger  $z$  these cases might turn the Universe into a deceleration mode, which is consistent with the behavior of the various quantities shown in Fig. 3. We can see that Case I gives the closest curve behavior to the one from the  $\Lambda$ CDM model. In Fig. 5, we demonstrate the possibility of the spin-zero connection fields accounting for the effect of dark energy with a suitable set of parameters and initial data. A comparison of Fig. 5 with the results in [2] shows that this two-scalar-mode model can give (not surprisingly) a better fitting of the supernova data than the one-scalar-mode model can.

## 7. Discussion

From a series of earlier works [16, 15, 17, 18] it was concluded that the Poincaré Gauge Theory of gravity has two good dynamic Lorentz connection modes, the “scalar” mode (spin  $0^+$ ) and the “pseudoscalar” mode (spin  $0^-$ ) which satisfy 2nd order equations.

Here we extended a previous work [2], which considered a PGT cosmological model with one dynamic Lorentz connection mode having spin  $0^+$ , to the case where both the scalar and pseudoscalar connection modes are dynamic. The objectives are (i) to study this PGT cosmological model (and in particular how well it can match the present universe observations) and (ii) to get a deeper understanding of the dynamics of the PGT.

From the cosmological homogeneous and isotropic assumptions the scalar and pseudoscalar curvatures  $R, E$  and the temporal components of the trace torsion  $f$  and axial torsion  $\chi$  survive and affect the evolution of the universe in this two-connection-mode model. Recognizing the equivalence of the model to one describing a particle with three degrees of freedom, we constructed an effective Lagrangian and the corresponding Hamiltonian by imposing the FLRW symmetry on the field theory action. The system of ODEs obtained therefrom are the same as the evolution equations obtained by imposing the FLRW symmetry on the equations derived from the PGT Lagrangian density.

With the evolution equations (24)–(29) and the associated energy constraint (30) we analyzed the late time asymptotic expansion. We found there are three normal modes: one related to the Hubble expansion and two dynamic modes represented by the torsion and curvature components. It was found that only the scalar mode affects the late-time expansion rate. The numerical analysis focused on the interaction between these two modes, the study of the possible behavior of the Universe, and the fitting to the observed supernova data. It was shown that the dynamical activity of the pseudoscalar mode could excite the scalar mode via the nonlinear coupling of these two modes, but the converse does not happen: one can have the scalar mode excited without any pseudoscalar excitation. Like the one-mode model in [2], the present model allows for an expanding universe with an oscillating component in

the expansion rate. Consequently, although on the average the expansion is slowing down, the universe can have an accelerating expansion at the present time. The additional degree of freedom in this two-mode model compared to the one in [2], not surprisingly, allows us to obtain a better fit to the supernova data.

From the evolution equations (26)–(29), we can see the nonlinear coupling between the scalar and pseudoscalar modes. In Sec. 6.1 we demonstrated the excitation of the scalar mode through the dynamical activity of the pseudoscalar mode. Such a nonlinear interaction between these two modes offers a natural mechanism to fuel the strength of the scalar mode in the evolution of the Universe. We stress that there is no known fundamental material source which directly excites the scalar mode; this part of the Lorentz connection simply does not interact in any obvious fashion with any familiar type of matter [21]. Conversely, the pseudoscalar mode is naturally driven by the intrinsic spin of fundamental fermions; in turn it naturally interacts with such sources. Indirectly, the  $0^+$  mode could be enhanced and activated dynamically through the aforementioned non-linear mechanism, in addition to any possible primordial amplitude from the early universe.

From the late-time analysis in Sec. 5, we showed that only the scalar mode, not the pseudoscalar mode, plays a direct role in affecting the expansion rate of the Universe. This result is perfectly consistent with our understanding of the characteristics of these two modes: Due to the ability of interacting with fermionic matter, it is generally thought that the axial torsion (controlled by the pseudoscalar part of the Lorentz connection) must be small and have small effects at the present time [19]. Conversely, the scalar Lorentz connection mode could be considered as a “phantom” field, at least in the matter-dominated epoch, since it will not interact directly with matter, and yet can drive the Universe in an oscillating fashion with an accelerating expansion at the present time.

As discussed in [2], the two Lorentz connection spin-zero modes in this model are in some ways effectively like a scalar field and a pseudoscalar field, yet these two “scalar” fields are fundamentally different from the various scalar field models of unknown matter, e.g., the quintessence models, in the following ways:

- this cosmological model is derived naturally from a geometric gravitational theory, the PGT, which is based on fundamental gauge principles, instead of on the hypothesis of the existence of a dark energy tailored to producing an explanation of an accelerating universe;
- there are, consequently, only a few free parameters in this cosmological model, instead of an ad hoc potential that can be rather arbitrarily chosen to fit the observations. Therefore, this PGT cosmological model should be more restrictive, and should be easier to be confirmed or falsified;
- based on its geometric character, the coupling of the dynamic parts of the Lorentz connection to the other fields is nothing like that which has ever been advocated for hypothetical scalar fields.

Thus this PGT cosmology with a Lorentz connection having dynamic “scalar” modes and the quintessence models are characteristically different, even though there are some similarities.

As mentioned in our previous work, if we consider the spacetimes as Riemannian instead of Riemann-Cartan, by absorbing the contribution of the post-Riemannian terms of this model into the stress-energy tensor on the rhs of the Einstein equations, as indicated in (33,34,35,36), then this contribution will act as a source of the Riemannian metric, effectively like an *exotic* fluid with its mass density  $\rho_\Gamma$  and pressure  $p_\Gamma$  varying with time (although the time evolution of these torsion and curvature terms are not like that of any fluid). Moreover, the effective fluid will appear to have presently a negative pressure, and consequently a negative parameter in the effective equation of state, i.e.,  $\omega_\Gamma \equiv p_\Gamma/\rho_\Gamma$ , which drives the universe into accelerating expansion. Note that there is no constraint on the value of  $\omega_\Gamma$  which appears here, and its value could vary from time to time. It should be stressed that this is not a real physical fluid situation; the truth is that  $\omega_\Gamma$  is nothing like “a connection field equation of state”, it is just a proportionality factor between  $\rho_\Gamma$  and  $p_\Gamma$ , two expressions which effectively summarize the contribution of the connection (via the curvature and torsion) acting as a source of the metric. The ratio  $\omega_\Gamma$  is of interest only to help understand the acceleration of this model and to enable a limited comparison with other dark energy proposals.

By imposing the FLRW symmetry on the Lagrangian density, we constructed an effective Lagrangian as well as the corresponding Hamiltonian. One benefit of the former is a simpler derivation of the dynamic equations (24)–(29). The latter should also prove useful, as the Hamiltonian formulation is the framework for the most powerful known techniques for analytically investigating the dynamics of a system. By these techniques one can to apply the experience accumulated in dealing with conservative classical mechanical systems. An effective Lagrangian and the corresponding Hamiltonian allows one to visualize the system as a particle moving in a potential. This would be very helpful in gaining a better appreciation of the dynamics of any sophisticated model. (Note, it is not necessarily true that an effective Lagrangian can be found in an arbitrary cosmological model. Extrapolating from GR, one can conjecture that this is possible for all PGT Class A Bianchi models with suitable sources, including pressure and spin). As we have seen in Sec. 5, the effective mechanical system methods were also useful for the late time normal mode analysis.

There have been some studies on PGT cosmology with dynamic scalar connection modes since the model proposed in [1, 2]. Wang and Wu [36] considered a related, but fundamentally different model, which turns out to have only the dynamic  $0^-$  mode. They considered the early universe and showed how in their model such a dynamic PGT connection could account for inflation (for another approach to using the PGT to account for inflation, see [31]). Li *et al.* [3, 4] presented a nice analysis of the scalar mode model of [2] from a more mathematical angle in order to get a deeper insight into the behavior of the dynamical system. In their work, they found the critical points of the system and the corresponding ranges of the parameters. In the latter work they also fit the model to the supernova data to find the best fit values of the parameters. These works considered quite general ranges of the parameters and found several interesting dynamical effects. We note that many of these interesting effects happen in parameter ranges which are outside of the restrictions considered by [2] to be physically necessary in order to have good linear modes (long ago [8, 13] the conditions were found so that the propagating modes should carry positive energy and satisfy the no-faster-than-light

condition). Also, a matter density of about 25% of the critical density was also imposed in [2] to give a more physical meaning to the a curve fitting. Further investigations and a careful study of the model will be needed to pin down the acceptable ranges of the parameters. In the present work, we have chosen the range of the related parameters following the result of [17] for good propagating scalar linear modes, just as in [2]. Applying the methods used in [3, 4] to the present extended model would surely lead to further insights.

One may wonder: how large must the post-Riemannian fields be in order to produce observable effects in the the present day universe, e.g., the observed acceleration? Conversely, how large can the torsion or curvature scalars be without violating some observational constraint? The questions merit a detailed study. Here is a simple argument that indicates a magnitude. Let us compare the terms in the Lagrangian density and the field equations for the model in which the PGT Lorentz connection has scalar dynamical modes and the Einstein theory with a cosmological constant. (In our present work we have deliberately included in most of the dynamical equations a possible cosmological constant; this was done not only for greater generality but also to facilitate just such a comparison. In our numerical evolution for our model we used  $\Lambda = 0$ .) Note that the presumed cosmological constant is “so small” that it has no noticeable effect in the laboratory, nor on the solar system scale, nor on the galactic scale. Nevertheless it is large enough to have the dominant effect on the cosmological scale. Hence we are led to infer that we should consider that one or more of the post-Riemannian terms ( $A_2 f^2$ ,  $A_3 \chi^2$ ,  $b^+ R^2$ ,  $b^- E^2$ ) should be comparable to the cosmological constant (which is about  $3\rho$ ) in the  $\Lambda$ CDM model. With such a choice we can expect that the post-Riemannian terms may be able to accelerate the universe and yet not be conspicuous on smaller scales.

The introduction of a new ingredient (i.e., the  $0^-$  connection mode which is reflected in the axial torsion and the pseudoscalar curvature) in this work raises the concern of the experimental and observational constraints on this field. There have also been some laboratory tests in search of torsion [40, 41]. The main idea among these experiments is the spin interaction between matter and torsion. The theoretical analyses and the high energy experimental data on four-fermion vertices sets the lower bound for the (pseudoscalar) torsion mass  $> 200$  Gev [19, 20, 21, 42]. The cosmological tests on torsion have investigated the effect of torsion-induced spin flips of neutrinos in the early Universe—which could alter the helium abundance and have other effects on the early nucleosynthesis [43, 44]. From Table 1, the parameters chosen for the range of the the torsion mass are consistent with the aforementioned analyses. Our model is also comfortable with the most restrictive experimental limits found on torsion [45]. For torsion being applied to the cosmological problem, Capozziello *et al.* [35, 46] have done a serious study on replacing the role of the cosmological constant in the accelerating Universe. With a totally antisymmetric torsion without dynamical evolution, their model is consistent with the observational data by tuning the amount of the torsion density. Compared with them, the model in this work allows the pseudoscalar torsion to evolve dynamically. This difference might enable a more fruitful physics to be studied.



## 8. Conclusion

In this work we considered the two “scalar” dynamical modes of the PGT Lorentz connection in a cosmological setting and have proposed it as a viable model for explaining the current status of the Universe. Besides seeking a better understanding of the PGT, we have considered the prospects of accounting for the outstanding present day mystery—the accelerating universe—in terms of an alternative gravity theory, more particularly in terms of the PGT with a dynamic Lorentz connection having only two dynamic modes, carrying spin-0 with even and odd parity. With the usual assumptions of isotropy and homogeneity in cosmology, we find that, under the model, the Universe will have with generic choices of the parameters an expansion rate which oscillates. The connection in this model could play the role of dark energy. With a certain range of parameter choices, it can account for the current status of the Universe, i.e., an accelerating expanding universe with a value of the Hubble constant which is approximately the present one. Thus we have considered the possibility that a certain geometric field, a dynamic Lorentz connection—which is naturally expected from spacetime gauge theory—could fully account for the accelerated universe.

The  $0^+$  mode, which directly drives the acceleration of the universe, does not couple directly to any known material source. By way of non-linear terms it could come indirectly from the huge density of the particles with sufficient spin alignment in the early universe which directly excite the  $0^-$  connection mode. The  $0^+$  mode could be considered as a “phantom” field, at least in the matter-dominated epoch, since it will not interact directly with matter; it only interacts indirectly via the gravitational equations. Then the dynamics of the scalar torsion mode could drive the Universe in an oscillating fashion with an accelerating expansion at present. It is quite remarkable that a gauge theory of dynamic geometry naturally presents us with such a “phantom” field. This natural geometric field could act like a dark energy.

## Acknowledgments

This work was supported in part by the National Science Council of the R.O.C. (Taiwan) under grant Nos. NSC97-2112-M-006-008, NSC97-2112-M-008-001. This work was also supported in part by the National Center of Theoretical Sciences and the (NCU) Center for Mathematics and Theoretical Physics. Some of the calculations were performed at the National Center for High-performance Computing in Taiwan. The encouragement and helpful advice of F. W. Hehl and C. Soo was much appreciated.

## Appendix A: The choice of parameters

Regarding our choice of parameters. From the table which can be found in any one of [15, 17, 18], we find that to kill the dynamics of the  $1^+$ ,  $2^+$ ,  $1^-$ ,  $2^-$  modes we want to take, respectively,

$$b_2 + b_5 = 0, \quad b_1 + b_4 = 0, \quad b_4 + b_5 = 0, \quad b_1 + b_2 = 0. \quad (84)$$

For dynamic  $0^+$  and  $0^-$  we want, respectively,

$$b_4 + b_6 > 0, \quad \text{and} \quad b_2 + b_3 < 0, \quad (85)$$

from Table 3 in [18]. Now, due to the Bach-Lanczos identity, we can choose any one of the parameters  $b_k$  to vanish. Taking, say  $b_4 = 0$  we then get that we also want  $b_1 = b_2 = b_5 = 0$ , leaving  $b_6 > 0$ ,  $b_3 < 0$ . We also find for the dynamic  $0^+$  and  $0^-$  modes, from Table 3 in [18] the respective restrictions

$$a_0 a_2 (2a_0 + a_2) < 0, \quad \text{and} \quad a_0 + 2a_3 < 0. \quad (86)$$

In terms of the parameters used in the present work, i.e.,

$$b^+ \equiv b_6, \quad b^- \equiv -b_3, \quad A_k \equiv -a_k, \quad m^+ \equiv A_0 + A_2/2, \quad m^- \equiv A_0 + 2A_3, \quad (87)$$

these restrictions become

$$b^+ > 0, \quad b^- > 0, \quad A_0 A_2 m^+ > 0, \quad m^- > 0. \quad (88)$$

The Newtonian limit gives  $A_0 = 1$ . A positive kinetic term in the action requires  $A_2 > 0$ .

In order to facilitate a comparison of the works of various groups, we here include the parameter conversion between those of the Cologne group of Hehl and coworkers (which we follow), Minkevich and coworkers [28, 29, 30, 31, 32], and Goenner and Müller-Hoissen [11]. In Hehl's work, the parameters related to the model described in this paper are  $a_0, a_2, a_3, b_3, b_6$ . Goenner and Müller-Hoissen used  $c_1 \cdots c_9$  as the parameters in their work. The Goenner and Müller-Hoissen parameters are related to Hehl's by

$$\begin{aligned} c_1 + 3c_2 &= \frac{a_3}{2}, \quad \sigma \equiv c_1 + 3c_3 = \frac{a_2}{2}, \quad c_4 = -\frac{a_0}{2}, \\ c_9 - c_8 &= \frac{b_3}{4}, \quad c \equiv 2(6c_5 + 2c_6 + 2c_7 - c_8 - c_9) = \frac{b_6}{2}, \end{aligned} \quad (89)$$

and thus

$$2c_4 - \sigma = m^+, \quad c_4 - 2c_1 - 6c_2 = \frac{m^-}{2}. \quad (90)$$

The parameters used by Minkevich are related to Hehl's by

$$b = a_3, \quad -\frac{a}{2} = a_2, \quad f_0 = -\frac{a_0}{2}, \quad q_2 = \frac{b_3}{4}, \quad q_1 = \frac{b_6 - b_3}{4}, \quad f = \frac{b_6}{8}, \quad (91)$$

and thus

$$2f_0 + \frac{a}{4} = m^+, \quad f_0 - b = \frac{m^-}{2}. \quad (92)$$

## References

- [1] Yo H J and Nester J M 2007 *Mod. Phys. Lett. A* **22** 2057.
- [2] Shie K F, Nester J M and Yo H J 2008 *Phys. Rev. D* **78** 023522.
- [3] Li X Z, Sun C B and Xi P 2009 *Phys. Rev. D* **79** 027301
- [4] Li X Z, Sun C B and Xi P 2009 *JCAP* **04** 015
- [5] Hehl F W, von der Heyde P, Kerlik G D and Nester J M 1976 *Rev. Mod. Phys.* **48** 393
- [6] Nester J M 1984 "Gravity, torsion and Gauge theory", in *Introduction to Kaluza-Klein theories*, ed H.C. Lee (World Scientific, Singapore), pp 83–115

- [7] Hehl F W 1980 in *Proc. of 6th Course of the International School of Cosmology and Gravitation on Spin, Torsion and Supergravity*, eds. P.G. Bergmann and V. de Sabbata (New York: Plenum) p5
- [8] Hayashi K and Shirafuji T 1980 *Prog. Theor. Phys.* **64** 866, 883, 1435, 2222
- [9] Mielke E W 1987 *Geometrodynamics of Gauge Fields* (Berlin: Akademie-Verlag)
- [10] Hehl F W, McCrea J D, Mielke E W and Neeman Y 1995 *Phys. Rep.* **258** 1
- [11] Gronwald F and Hehl F W 1996 “On the Gauge Aspects of Gravity” in *Proc. 14th Course of the School of Gravitation and Cosmology (Erice)*, ed. P.G. Bergman, V. de Sabata, and H.J. Treder (Singapore: World Scientific) pp 148–98.
- [12] Blagojević M 2002 *Gravitation and Gauge Symmetries* (Bristol: Institute of Physics).
- [13] Sezgin E and van Nievenhuizen P 1980 *Phys. Rev. D* **21** 3269
- [14] Blagojević M and Nicolici I A 1983 *Phys. Rev. D* **28** 2455
- [15] Chen H, Nester J M and Yo H J 1998 *Acta Phys. Pol. B* **29** 961
- [16] Hecht R, Nester J M and Zhytnikov V V 1996 *Phys. Lett. A* **222** 37
- [17] Yo H J and Nester J M 1999 *Int. J. Mod. Phys. D* **8** 459
- [18] Yo H J and Nester J M 2002 *Int. J. Mod. Phys. D* **11** 747
- [19] Carroll S M and Field G B 1994 *Phys. Rev. D* **50** 3867
- [20] Belyaev A S and Shapiro I L 1999 *Nucl. Phys. B* **543** 20
- [21] Shapiro I L 2002 *Phys. Rep.* **357** 113
- [22] Peebles P J E and Ratra B 2003 *Rev. Mod. Phys.* **75** 559
- [23] Padmanabhan T 2003 *Phys. Rep.* **380** 235
- [24] Copeland E J, Sami M and Tsujikawa S 2006 *Int. J. Mod. Phys. D* **15** 1753
- [25] Caldwell R R, Dave R and Steinhardt P J 1998 *Phys. Rev. Lett.* **80** 1582
- [26] Carroll S M 1998 *Phys. Rev. Lett.* **81** 3067
- [27] Balaji K R S and Brandenberger R H 2005 *Phys. Rev. Lett.* **94** 031301
- [28] Minkevich A V 1980 *Phys. Lett. A* **80** 232
- [29] Minkevich A V 1983 *Phys. Lett. A* **95** 422
- [30] Minkevich A V and Nemenman I M 1995 *Class. Quantum Grav.* **12** 1259
- [31] Minkevich A V and Garkun A S 2006 *Class. Quantum Grav.* **23** 4237
- [32] Minkevich A V, Garkun A S and Kudin V I 2007 *Class. Quantum Grav.* **24** 5835
- [33] Goenner H and Müller-Hoissen F 1984 *Class. Quantum Grav.* **1** 651
- [34] Böhmer C 2004 *Class. Quantum Grav.* **21** 1119; 2005 *Acta Phys. Polon. B* **36** 2841
- [35] Capozziello S, Carloni S and Troisi A 2003 *Recent Res. Dev. Astron. Astrophys.* **1** 625
- [36] Wang C H and Wu Y H 2009 *Class. Quantum Grav.* **26** 045016.
- [37] Ashetkar A and Samuel J 1991 *Class. Quantum Grav.* **8** 2191
- [38] Riess A G, *et al.* 2004 *Astrophys. J.* **607** 665
- [39] Riess A G, *et al.* 1998 *Astron. J.* **116** 1009; Perlmutter S, *et al.* 1999 *Astrophys. J.* **517** 565
- [40] Chui T C P and Ni W T 1993 *Phys. Rev. Lett.* **71** 3247
- [41] Ni W T 1996 *Class. Quantum Grav.* **13** A135
- [42] Chang L N and Soo C 2003 *Class. Quantum Grav.* **20** 1379
- [43] Capozziello S, Iovane G, Lambiase G and Stornaiolo C 1999 *Europhys. Lett.* **46** 710
- [44] Brüggen M 1999 *Gen. Rel. Grav.* **31** 1935
- [45] Kostelecky V A, Russell N, and Tasson J D 2008 *Phys. Rev. Lett.* **100** 111102
- [46] Capozziello S, Cardone V F, Piedipalumbo E, Sereno M and Troisi A 2003 *Int. J. Mod. Phys. D* **12** 381